The Stability of Nonlinear Systems in the Region of Linear Dominance

I. A. GURA and D. D. PERLMUTTER

University of Illinois, Urbana, Illinois

A technique has been developed for finding quantitative regions of asymptotic stability for nonlinear systems by using a known proof of the theorem which substantiates the linearization. In a sense, the method defines a region in which the first-order approximation is dominant from the point of view of stability. While the computations necessary can be somewhat involved, the procedure is essentially identical in all situations, and once established, can easily be used for a vast class of autonomous systems. The practical problems of both reversible and irreversible chemical reactions occurring in a continuous flow stirred vessel have been analyzed. Stability regions were obtained which are sufficiently extensive to be practical from the process viewpoint.

PART I

The analysis and design of control systems have given practical engineering importance to the mathematical theorems having to do with the stability of ordinary differential equations. For linear systems a variety of techniques are available for graphical or analytic solutions. Developments for nonlinear systems in particular have followed either of two paths. By the direct method, a Liapunov function is sought which will be sufficient to establish a region of asymptotic stability in phase space. This approach utilizes the precise nature of the nonlinearity and may yield global results. However, an important drawback is the lack of a systematic, widely applicable procedure; usable engineering results for each new problem still depend on the ingenuity of the investigator, although a number of generalizations have been made (*6, 8*).

Alternatively, the stability of a nonlinear system may be related to the stability of a more tractable linear system. This linearization, sometimes called Liapunov's first method, is based on the expectation that first-order approximations can adequately describe the behavior of the nonlinear functions. Strictly speaking, this is valid only for small deviations from the point of linearization; as commonly formulated (*2, 9, 10*), the stability established in this way is local stability in some neighborhood of unknown size. Results based on such considerations are of limited use because of their qualitative nature.

In this paper it will be shown that quantitative results of practical significance can be obtained from these ideas. In effect, a region will be determined so that for all initial conditions within its boundary, the linearized version of a nonlinear differential equation will be dominant from the point of view of stability. Since the necessary and sufficient conditions for the stability of linear systems are well known, the method is systematic and applicable to a very wide class of nonlinear problems.

THE FUNDAMENTAL THEOREM

Consider a system that can be written as the vector equation

$$\dot{\mathbf{x}} = \mathbf{F}(\mathbf{x}) = \mathbf{J}_s\,[\mathbf{x} - \mathbf{x}_s] + \mathbf{f}(\mathbf{x}) \qquad (1)$$

where $\mathbf{F}$ is a vector function possessing continuous first-order partial derivatives in some neighborhood of $\mathbf{x}_s$, the steady state of interest, and $\mathbf{J}_s$ is the Jacobian matrix $[\partial F_i/\partial x_j]$ evaluated at the steady state. By defining $\mathbf{y} = \mathbf{x} - \mathbf{x}_s$, the linearized version of (1) is

$$\dot{\mathbf{y}} = \mathbf{J}_s\,\mathbf{y} \qquad (2)$$

Equation (2) can also be put in the form

$$\mathbf{y} = \psi(t)\mathbf{y}(0) + \int_0^t \psi(t-s)\mathbf{f}(s)\,ds \qquad (3)$$

where the function $\psi(t)$ is the principal matrix solution (*10*), namely, the unique matrix satisfying

$$\dot{\psi} = \mathbf{J}_s\,\psi,\ \psi(0) = \mathbf{I} \qquad (4)$$

The fundamental theorem of stability (*2, 9, 10*) states that if the linear approximation (2) is asymptotically stable at $\mathbf{x}_s$, then the nonlinear system (1) must be asymptotically stable in some region about $\mathbf{x}_s$. Indeed, for every $\epsilon > 0$, there exists a $\delta > 0$, such that $||\mathbf{y}(t)|| \leq \delta$ implies

$$\frac{||\mathbf{f}(\mathbf{y}(t) + \mathbf{x}_s)||}{||\mathbf{y}(t)||} \leq \epsilon \qquad (5)$$

Moreover, the definition of stability requires that for every $\delta > 0$, there exists an $R > 0$, such that $||\mathbf{y}(0)|| \leq R$ implies $||\mathbf{y}(t)|| \leq \delta$ for all $t \geq 0$. The relationships between R, δ, and ϵ can most readily be summarized by a two-dimensional geometric argument. A choice of ϵ defines a region about the steady state in the (y_1, y_2) plane for which Equation (5) is fulfilled. The curves $||\mathbf{y}(t)|| =$ constant are closed contours in this region. That constant which gives the largest contour wholly within the ϵ region is the desired value of δ. The stability region is within the smaller concentric contour given by $||\mathbf{y}(0)|| = R$. All trajectories resulting from such initial conditions will be bounded by $||\mathbf{y}(t)|| < \delta$ and will eventually decay to the steady state. For higher order systems, the above arguments are the same except that δ and R will be given by appropriate n-dimensional surfaces.

Since the stability regions established in this manner are defined by norms, they will differ in size and shape, depending on the norm used. The method developed here is valid for the general Hölder norm

$$||\mathbf{A}|| = \left(\sum_{i=1}^{n} \sum_{j=1}^{m} |a_{ij}|^p \right)^{1/p} \qquad (6)$$

I. A. Gura is with Hughes Aircraft Company, Culver City, California, and D. D. Perlmutter is with the University of Pennsylvania, Philadelphia, Pennsylvania.

Some common examples of (6) are

diamond norm, $p = 1$

$$||\mathbf{A}||_d = \sum_{i=1}^{n} \sum_{j=1}^{m} |a_{ij}| \tag{6a}$$

Euclidian norm, $p = 2$

$$||\mathbf{A}||_e = \left[\sum_{i=1}^{n} \sum_{j=1}^{m} |a_{ij}|^2 \right]^{1/2} \tag{6b}$$

square norm, $p = +\infty$

$$||\mathbf{A}||_{sq} = \max_{i,j} |a_{ij}| \tag{6c}$$

Furthermore, it is not necessary that the regions of stability be regular in shape. It would be advantageous to try various transformations

$$\mathbf{u}(t) = \mathbf{B}\mathbf{y}(t) \tag{7}$$

so as to maximize this region.

Although the number of feasible transformations is limitless, several well-chosen possibilities usually suffice to indicate the order of magnitude of the largest stability region that can be found from the fundamental theorem. Hence, little loss of generality will be encountered if the transformations used are limited to rotations followed by expansions or contractions of coordinates. The transformation matrix $\mathbf{B}$ can then be expressed as

$$\mathbf{B} = \begin{bmatrix} b_1 & 0 \\ 0 & b_2 \end{bmatrix} \begin{bmatrix} \cos\theta & \sin\theta \\ -\sin\theta & \cos\theta \end{bmatrix} \tag{8}$$

where θ is the angle of rotation and the constants b_1 and b_2 define the scale change. The choice of coordinates used for a given problem is closely related to the choice of norm used and a search for maximum stability regions can be performed from either viewpoint.

BOUNDING THE PRINCIPAL MATRIX SOLUTION

In general, if (2) is stable there exist positive constants c and q such that

$$||\psi(t)|| \leq ce^{-qt} \tag{9}$$

These constants can be chosen freely within constraints imposed by the linear system (2). In the following these constants will be used to establish numerical regions of proved stability by letting $\epsilon = (q/kc)$, where, depending on the norm used, k is the constant which satisfies

$$||\mathbf{AB}|| \leq k\,||\mathbf{A}||\;||\mathbf{B}|| \tag{10}$$

For the common norms defined above the k's are unity for the Euclidian and diamond norms, and equal to the dimension of j for the square norm. The largest possible δ is given by the $||\mathbf{y}(t)||$ that satisfies

$$\frac{||\mathbf{f}(\mathbf{y}(t) + \mathbf{x}_s)||}{||\mathbf{y}(t)||} = \frac{q}{kc} \tag{11}$$

and consequently

$$||\mathbf{y}(0)|| < \frac{\delta}{kc} = R \tag{12}$$

Since the constants c and q are used to find the largest region about the steady state that satisfies (11), it is apparent that q and c should be chosen so as to maximize the ratio q/c. These constants are not completely arbitrary. The value of q must always be less than q_o, the absolute value of the largest real part of the characteristic roots, while the value of c is bounded from below since $\psi(0) = \mathbf{I}$ and $||\mathbf{I}|| \leq c$ must be satisfied (*10*). The particular bound on c depends on the norm chosen and the order of the system, n. For example, c for the diamond norm cannot be less than n. For the Euclidian norm, it cannot be less than the square root of n, and for the square norm, its smallest possible value is unity. Since the bounds on q and c are in opposing directions, an optimum is desired. Although the various elements of $\psi(t)$ can be found by linear techniques, it is not a simple matter to find the maximum (q/c) analytically. Direct numerical calculation is probably the best approach to a solution of the problem.

The first step is to find the values of the elements of $\psi(t)$ at various intervals from $t = 0$ to the point where the dominant exponential of $\psi(t)$ has decayed to approximately 1% of its initial value. This can be accomplished from analytic formulas for $\psi(t)$, or by solution of the linear equations involved by any common numerical technique. Once $||\psi(t)||$ is known at each t, various possibilities for c and q can be tested to see if the corresponding ce^{-qt} is a valid bound. Although it is not generally the case, $||\psi(t)||$ can sometimes be bounded by ce^{-qt} with q at q_o, its maximum permissible value, and c at its minimum value for the norm chosen. This case is tested first, and if it is successful the problem is solved. If it fails, however, a systematic method of testing combinations of q's and c's must be employed.

The key to such a computational scheme lies in studying

$$\log ||\psi(t)|| \leq -qt + \log c \tag{13}$$

instead of (9). From this viewpoint, the functional bounds desired are now straight lines, which in many situations can be taken as the various tangents to $\log ||\psi(t)||$. The slope of $\log ||\psi(t)||$ vs. t at each point is

$$q_1 = \frac{\dfrac{d\,||\psi(t)||}{dt}}{||\psi(t)||} \tag{14}$$

Those slopes which lie in the range $-q_o \leq q_1 \leq 0$ are retained and since each of them corresponds to a tangent line, the related c can be found in every case by extrapolating that line to $t = 0$. Thus $a(q/c)$ can be found wherever the slope of $\log ||\psi(t)||$ is applicable to a bounding function. The maximum of these ratios is located, and the corresponding ce^{-qt} is tested at each t to see if it does indeed bound $||\psi(t)||$. If it does not, the same calculation is carried out for the second largest (q/c), and so on. This procedure will converge to an answer in most cases, but because of the discrete nature of the calculations, it is possible that none of the functions tested will bound $||\psi(t)||$. This can occur, for example, if $||\psi(t)||$ has a sharp peak and points near the summit are skipped. In such a situation the intervals of time can be reduced, and the entire calculation repeated.

A program may be developed that can be adapted to any norm and any order system for which the elements of the system matrix are the only input data necessary. If $\mathbf{BJ}_s\mathbf{B}^{-1}$ is used as the system matrix for transformed coordinates, the program can be used in the search over $\mathbf{B}$ for the optimum stability region.

SUMMARY OF PROCEDURE

The major steps in finding a region of asymptotic stability may be summarized as follows

1. Establish the local stability of the steady state by examining the real parts of the characteristic roots of the linearized set of Equations (2). If all are negative, the system is locally stable and the analysis can be continued.

2. Decide on a set of transformation matrices to be used in the search for an optimal stability region. For a second-order problem use Equation (8).

3. Note the value of the largest real part of the characteristic roots of (2) and thus establish the maximum q permissible for use in bounding the principal matrix (q_o).

4. Find the various functions $f_1, f_2, \ldots, f_n$ from the formula (5)

$$f_i(\mathbf{x}) = g_i(\mathbf{x}) - g_i(\mathbf{x}_s) - \sum_{j=1}^{n} \frac{\partial g_i}{\partial x_j}(x_j - x_{js}) \quad (15)$$

5. Choose a norm to use in solving the problem and write an expression for

$$\frac{||\mathbf{Bf}(\mathbf{B}^{-1}\mathbf{u}(t) + \mathbf{x}_s)||}{||\mathbf{u}(t)||}$$

6. Use an appropriate computer program to find

(a) the values of q and c so that Equation (8) is satisfied and q/c is a maximum,

(b) the trajectory bound δ implied by

$$\frac{||\mathbf{Bf}(\mathbf{B}^{-1}\mathbf{u}(t) + \mathbf{x}_s)||}{||\mathbf{u}(t)||} < \frac{q}{kc} \quad (16)$$

and the stability region implied by

$$||\mathbf{u}(0)|| < \frac{\delta}{kc} \quad (17)$$

Two computational algorithms based on interval halving techniques were used to find the stability region implied by (17). The first method establishes the boundary of validity of (16) by a series of one-dimensional searches along paths parallel to one of the coordinate axes. Whenever a step in the search procedure causes a violation of (16), the step size is halved and its sign is reversed. The boundaries of the region for which (16) holds are graphed, and, as appropriate, the largest square, circle, or diamond is inscribed. This determines the trajectory bound δ in each case. By diminishing its size by the factor (kc), the desired region of stability is found.

The alternative procedure, which finds the δ region directly and bypasses the explicit calculation of the ϵ condition boundary, follows a search around the perimeter of the inscribed curve (or surface). For the two-dimensional Euclidian norm, for example, a circle which lies wholly in the region of (16) is desired as a first step. This can be obtained by successive reduction of any initial radius until one is found for which (16) is satisfied at all angles between 0 and 2π. Once this circle and any other circle that intersects the boundary of (16) are known, an interval halving technique can be used to progressively reduce the difference between the radius of the circle within the region and the one partially outside. The problem can be solved to any desired degree of accuracy. The answer is then divided by the appropriate (kc) to give the actual stability region.

PART II

To establish that the foregoing procedures do indeed yield regions of stability that are of practical interest, it is necessary to examine numerically applications to significant engineering problems. A stability study of various chemical reactor models was carried out, in part because of its intrinsic interest to chemical engineers, but also to enable comparisons with earlier work. The most complete linearized treatment to date of the control and stability problems for a well-stirred reactor is that of Aris and Amundson (*1*). The stability of various steady states was examined in that work. Hoftyzer and Zwietering (*7*) followed the same procedure with the dynamic equations for the polymerization of ethylene. For the analysis of the effect of nonlinearities in the large, Warden, Aris, and Amundson (*11*) and Berger and Perlmutter (*3, 4*) constructed Liapunov functions. The system parameters used in the present work were chosen from one of the examples in the latter reference so that direct comparisons can be made.

TEMPERATURE-DEPENDENT, IRREVERSIBLE REACTION

Consider an irreversible homogeneous reaction occurring in a continuous flow well-stirred vessel. The dynamics of the system are described by an energy and a mass balance.

$$\left.\begin{aligned} \rho V C_p \frac{dT}{dt} &= \Delta H V r - U A_r (T - T_a) - \rho Q C_p (T - T_o) \\ V \frac{dC}{dt} &= -Vr - Q(C - C_o) \end{aligned}\right\} \quad (18)$$

Assume a first-order reaction governed by an Arrhenius temperature dependence so that

$$r = Ck_o e^{-E/RT} \quad (19)$$

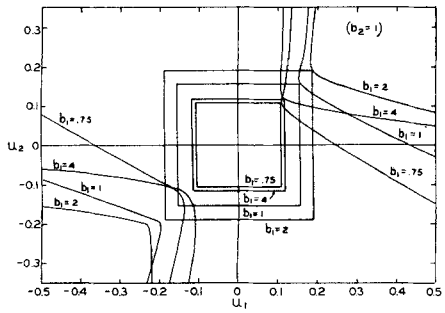

Fig. 1. Temperature-dependent reactor; ϵ conditions for the square norm.

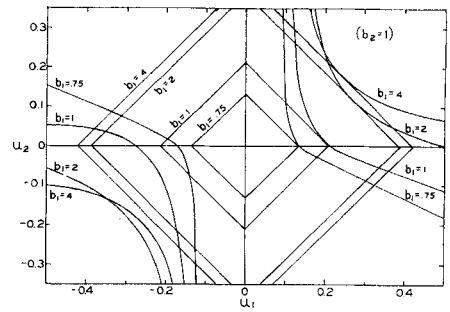

Fig. 2. Temperature-dependent reactor; ϵ conditions for the diamond norm.

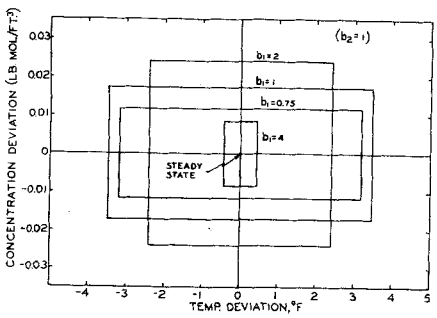

Fig. 3. Temperature-dependent reactor; stability regions for the square norm.

The system equations (18) can be normalized and abbreviated by defining the state variables

$$\left.\begin{aligned} x_1 &= \rho C_p T/\Delta H C_o \\ x_2 &= C/C_o \end{aligned}\right\} \tag{20}$$

and the constants

$$\left.\begin{aligned} k_1 &= -E\rho C_p/R\Delta H C_o \\ k_2 &= (UA_r + \rho Q C_p)/\rho V C_p \\ k_3 &= (T_o UA_r + \rho C_p T_o Q)/\Delta H V C_o \\ k_4 &= Q/V \end{aligned}\right\} \tag{21}$$

Substituting in (16) and combining with (17) results in

$$\left.\begin{aligned} \frac{dx_1}{dt} &= x_2 k_o\, e^{(k_1/x_1)} - k_2 x_1 + k_3 \\ \frac{dx_2}{dt} &= -x_2 k_o\, e^{(k_1/x_1)} - k_4 x_2 + k_4 \end{aligned}\right\} \tag{22}$$

A similar procedure was followed in simplifying Equation (18) in the earlier references cited. To specify a particular stability problem, the following system parameters were chosen: $k_o = 10^9$ hr.$^{-1}$; $E/R = 10^4$ °R.; $U = 5$ B.t.u./sq.ft. °F.; $A_r = 100$ sq.ft.; $V = 100$ cu.ft.; $C_o = 0.270$ lb. mole/cu.ft.; $C_p = 1.0$ B.t.u./lb. °F.; $\rho = 50$ lb./cu.ft.; $T_o = T_A = 530$ °R.; $\Delta H = 10^4$ B.t.u./lb. mole; $Q = 200$ cu.ft./hr.

For these constants the only steady state of (22) in the region of physical significance (460° to 1,500°R.) is at $T_s = 550$°R. ($x_{1s} = 10.2$), $C_s = 0.165$ lb. mole/cu.ft. ($x_{2s} = 0.612$).

The elements in the Jacobian matrix for the system (22) are

$$\left.\begin{aligned} j_{11} &= \frac{-k_1}{x_1^2} k_o x_2 \exp(k_1/x_1) - k_2 \\ j_{12} &= k_o \exp(k_1/x_1) \\ j_{21} &= \frac{k_1 k_o}{x_1^2} x_2 \exp(k_1/x_1) \\ j_{22} &= -k_o \exp(k_1/x_1) - k_4 \end{aligned}\right\} \tag{23}$$

These functions are continuous everywhere except at $x_1 = 0$. Since that point corresponds to absolute zero on the temperature scale, this limitation is unimportant. For the particular system under consideration, the real parts of the characteristic roots of J_s are negative, thus assuring the local stability of the steady state in question. By Equation (15)

$$\left.\begin{aligned} f_1(\mathbf{x}) &= x_2 k_o \exp(k_1/x_1) - \\ &\quad k_o \exp(k_1/x_{1s}) \left[x_2 - \frac{k_1 x_{2s}}{x_{1s}^2}(x_1 - x_{1s}) \right] \\ f_2(\mathbf{x}) &= -f_1(\mathbf{x}) \end{aligned}\right\} \tag{24}$$

and

$$f_1(\mathbf{y} + \mathbf{x}_s) = (y_2 + x_{2s}) k_o \exp(k_1/(y_1 + x_{1s})) - k_o \exp(k_1/x_{1s}) \left[y_2 + x_{2s} - \frac{k_1 x_{2s}}{x_{1s}^2} y_1 \right] = -f_2 \tag{25}$$

Expansion of Coordinates

The stability problem was first solved using a simple diagonal matrix for **B**; that is, by letting the angle of rotation $\theta = 0$. Then from (8) and (25)

$$f_1(\mathbf{B}^{-1}\mathbf{u} + \mathbf{x}_s) = (u_2/b_2 + x_{2s}) k_o \exp\left(\frac{k_1}{u_1/b_1 + x_{1s}}\right) - k_o \exp(k_1/x_{1s}) \left([u_2/b_2 + x_{2s}] - \frac{k_1 x_{2s} u_1}{x_{1s}^2 b_1} \right) = -f_2 \tag{26}$$

The ϵ condition for the square norm is

$$\frac{||\mathbf{B}\mathbf{f}(\mathbf{B}^{-1}\mathbf{u} + \mathbf{x}_s)||_{sq}}{||\mathbf{u}||_{sq}} = \frac{\max[|b_1|, |b_2|]\, |f_1(\mathbf{B}^{-1}\mathbf{u} + \mathbf{x}_s)|}{\max[|u_1|, |u_2|]} < \left(\frac{q}{2c}\right)_{sq} \tag{27}$$

and similarly for the diamond norm

$$\frac{[|b_1| + |b_2|]\, |f_1(\mathbf{B}^{-1}\mathbf{u} + \mathbf{x}_s)|}{|u_1| + |u_2|} < \left(\frac{q}{c}\right)_d \tag{28}$$

The boundaries of validity of (27, 28) were found computationally for several values of b_1 with $b_2 = 1$ in each case. These are shown in Figures 1 and 2 along with the largest squares and diamonds that can be inscribed in these regions. By inverse transformation and application of the δ condition, the corresponding stability regions are found in temperature-concentration coordinates. The results are indicated in Figures 3 and 4. It is important to note from Figures 3 and 4 that the regions for $b_1 = 4$ and 0.75 are totally within other stability regions for which b_1 is between these extremes. There is, therefore, a limit to what can be gained by varying b_1. Similarly, variation in b_2 will not improve the results already obtained. This result is intuitively expected, for the linear dominance should become ineffective somewhere in every coordinate system.

Comparisons among Norms

If **B** is set equal to the identity matrix, the various norms can be compared in the absence of any coordinate transformation. This was done to obtain the results of Table 1. In this table, and those that follow, ΔT_{max} and ΔC_{max} are the maximum permissible deviations from the steady state, as measured by the projection of the stability region on the respective axes. Comparing the results for the diamond and Euclidian norms without transformation, it is seen that the stability region found with the latter is much larger. This effect can be explained by consider-

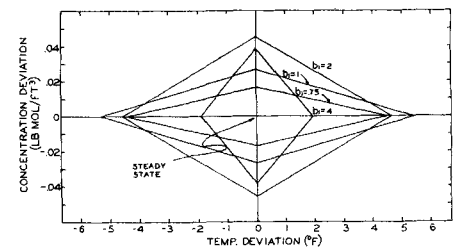

Fig. 4. Temperature-dependent reactor; stability regions for the diamond norm.

Table 1. Comparison Among Norms for Temperature Dependent Reactor

Norm	c	kc	q	q/kc	ΔT_{max}	ΔC_{max}
Square	1.21	2.42	1.38	0.571	3.5	0.017
Diamond	2.15	2.15	1.12	0.523	5.3	0.026
Euclidian	1.42	1.42	1.28	0.906	11.4	0.057

ing the quantity kc used in bounding $\psi(t)$ in each case. This factor is crucial in determining the results, since the size of the regions described by both the ϵ and δ conditions varies inversely with the magnitude of kc. While the minimum value of kc is 2 for the diamond and square norms, it is $\sqrt{2}$ for the Euclidian norm. Hence, larger stability regions would be expected with the Euclidian norm. The results substantiate this argument, as indicated in Table 1.

General Linear Transformation

Since the stability regions obtained so far are relatively small, the Euclidian norm is considered in conjunction with the general transformation matrix of Equation (8). For each choice of b_1, b_2, and θ, and elliptical stability region results in temperature-concentration coordinates. Several representative results are shown in full in Figure 5; the corresponding transformation parameters are in Table 2. Some of the stability regions are quite large from a practical standpoint, while others are extremely small. The method is evidentally very dependent on the proper choice of coordinates.

Feedback Control

The effect of proportional feedback control offers an interesting extension to the problem of the well-stirred reactor. As an example, let the feed temperature and feed concentration be described as the following functions of reactor conditions.

$$T_o = T_o' + K_t\,(T - T_s) \tag{29}$$

$$C_o = C_o' + K_c\,(C - C_s) \tag{30}$$

Substituting these relationships in Equation (18) results in the new system equations

$$\rho V C_p \frac{dT}{dt} = \Delta H V_r - UA_r\,(T - T_a)$$

$$-\rho Q C_p\,[T - T_o' - K_t\,(T - T_s)] \tag{31}$$

$$V\frac{dC}{dt} = Vr - Q[C - C_o' - K_c\,(C - C_s)]$$

By a procedure analogous to that followed previously, these equations can be transformed to x space. The only differences between the uncontrolled and controlled cases

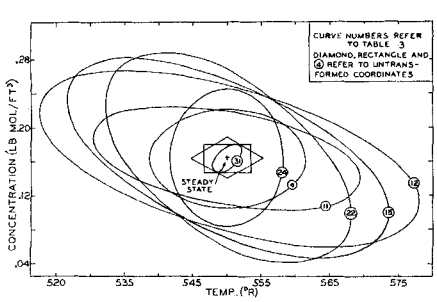

Fig. 5. Temperature-dependent reactor; stability regions for generalized Euclidian norm.

Table 2. Transformation Parameters: Temperature-Dependent Reactor Using the Euclidian Norm

Computation number	b_1	b_2	θ
4	1	1	0
11	1	2	−20
12	1	2	−30
15	1	2	−45
22	1	2	−60
24	1	2	−90
31	1	2	+60

are the additional linear terms which appear in the latter system. Hence, once the Jacobian matrix is accordingly modified, the remainder of the stability analysis must follow as before. Some results of using various combinations of K_t and K_c are shown in Table 3; a more complete tabulation is in Reference (5). All calculations were performed with $b_1 = 1$, $b_2 = 2$, $\theta = 45$ deg., since this transformation results in a relatively large stability region even when no control is used. It may be noted from the table that the proved stability region is reduced by use of concentration control alone, while it is enlarged with temperature control and with temperature and concentration control used together. In all cases, the stability region depends directly on the calculated ratio q/c. This is expected because q/c is the only quantity in the ϵ condition that is affected by linear control.

As seen from Table 3, increasingly negative K_t produces enlarged stability regions; however, the same does not hold true for K_c. In fact, for each K_t the maximum region occurs at a value of K_c, which is not the largest shown. In any case, these constants cannot be increased indefinitely for resulting control functions may not be physically practical. Several selected results are shown in Figure 6, where the effect of control is apparent. Only two controlled cases are shown since they are fairly representative of all the regions indicated in Table 3.

From the physical limitations of the system, the temperature in the reactor cannot be less than the feed temperature, and the concentration must always be somewhere between that of the feed and zero. By this argument, any trajectory originating in the shaded area in Figure 6 must move away from the dotted boundaries for the controlled cases shown. Since these trajectories must at some time enter a region of asymptotic stability, the shaded area itself must be a region of asymptotic stability. Thus, the controlled reactors are stable from start-up conditions.

Table 3. Typical Stability Results for A Controlled Temperature-Dependent Reactor

$-K_t$	$-K_c$	q/c	ΔT_{max}	ΔC_{max}
0.0*	0	1.19	23.5	0.117
2.5*	0	2.17	33.8	0.169
3.0	0	2.21	34.0	0.170
0.0	1.0	0.806	18.0	0.090
0.0	3.0	0.654	15.5	0.077
1.0	1.0	1.96	22.5	0.111
1.0	3.0	2.12	33.3	0.167
1.5	1.5	2.70	29.1	0.146
1.5	2.0	3.05	40.4	0.202
1.5	3.0	2.87	39.2	0.196
2.0	1.0	2.91	32.6	0.163
2.0*	1.5	3.87	45.4	0.227
2.0	3.0	3.64	44.2	0.221

* Shown in Figure 6.

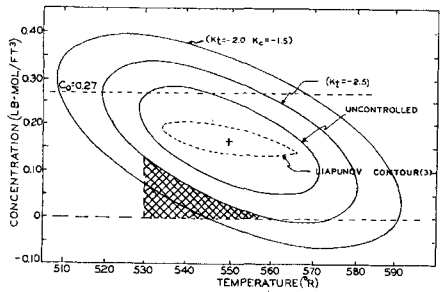

Fig. 6. Temperature-dependent reactor; comparison of stability regions.

The same generalization does not apply to the uncontrolled case, because trajectories originating in the shaded area do not have to enter the established stability region.

The dotted curve in Figure 6 was found via Liapunov's direct method (3) for the same system. By comparison, it encloses a much smaller region than the ones found from the fundamental theorem. In a later work (4), the same authors were able to extend the region considerably by generalizing the functions used. It may be added, however, that the regions shown in Figure 6 are sufficient for many practical purposes.

REVERSIBLE ISOTHERMAL REACTION

An important limitation to the method presented here may be emphasized by a study of a reversible reaction. To analyze the effects of reversibility and yet avoid the complications of a third-order system, the temperature dependence can be omitted. Physically, this is justified if temperature control is rapid and very accurate. Consider the chemical reaction

$$\alpha A + \alpha_1 A_1 + \alpha_2 A_2 + \ldots \rightleftharpoons \beta B + \beta_1 B_1 + \beta_2 B_2 + \ldots$$

If the feed to the reactor contains the components A, A_1, A_2 in stoichiometric proportions, the dynamics of a continuous flow, well-stirred reactor can be expressed by two mass balances

$$\left.\begin{aligned} V\frac{dC_A}{dt} &= -Vr - Q(C_A - C_{Ao}) \\ V\frac{dC_B}{dt} &= \frac{\beta}{\alpha}Vr - Q(C_B - C_{Bo}) \end{aligned}\right\} \quad (32)$$

Assume a reaction rate of the form

$$r = K_F C_A^{\,n} - K_R C_B^{\,m} \quad (33)$$

Define the state variables

$$x_1 = C_A, \quad x_2 = C_B$$

and the constant $\tau = V/Q$. The system equations become

$$\left.\begin{aligned} \frac{dx_1}{dt} &= -K_F x_1^{\,n} + K_R x_2^{\,m} - \frac{1}{\tau}(x_1 - x_{1o}) \\ \frac{dx_2}{dt} &= \frac{\beta}{\alpha}K_F x_1^{\,n} - \frac{\beta}{\alpha}K_R x_2^{\,m} - \frac{1}{\tau}(x_2 - x_{2o}) \end{aligned}\right\} \quad (34)$$

The Jacobian matrix for this system is

$$\mathbf{J} = \begin{bmatrix} -K_F n x_1^{\,n-1} - \frac{1}{\tau} & K_R m x_2^{\,m-1} \\ \frac{\rho}{\alpha}K_F n x_1^{\,n-1} & -\frac{\beta}{\alpha}K_R m x_2^{\,m-1} - \frac{1}{\tau} \end{bmatrix} \quad (35)$$

The elements of this matrix are continuous everywhere for positive integral values of m and n. If, however, m and n are nonintegral, the Jacobian matrix exists in the real sense only when x_1 and x_2 are not negative. This is an example of the limitation on linearization. By Equation (15)

$$f_1(\mathbf{x}) = -K_F x_1^{\,n} + K_R x_2^{\,m} + K_F x_{1s}^{\,n} - K_R x_{2s}^{\,m} + K_F n x_{1s}^{\,n-1}(x_1 - x_{1s}) - K_R m x_{2s}^{\,m-1}(x_2 - x_{2s}) = -\frac{\alpha}{\beta}f_2(\mathbf{x}) \quad (36)$$

From this, the ϵ conditions for the diamond, square, and Euclidian norms can be found as before.

Consider now the specific case for which $\tau = 0.40$ hr.; $C_{Bo} = 0.0$ lb. mole/cu.ft.; $C_{Ao} = 0.270$ lb. mole/cu.ft.; $\beta/\alpha = 1$; $K_F = 1.00$ [lb. mole/cu.ft.]$^{1/2}$/hr.; $K_R = 0.20$ [lb. mole/cu.ft.]$^{1/2}$/hr.; $m = 0.5$; $n = 0.5$. In the range of interest the only steady state for this reactor is $C_{As} = 0.146$, $C_{Bs} = 0.124$; for this steady state the linearized version of (32) is asymptotically stable and the fundamental theorem can be applied. From (34)

$$f_1(\mathbf{x}) = -\sqrt{x_1} + 0.2\sqrt{x_2} + 1.31(x_1 - .27) - 0.284x_2 + 0.312 = -f_2(\mathbf{x}) \quad (37)$$

These functions are not real for any x_1 or x_2 less than zero. Thus, a search for the boundary of validity of Equation (9) must not cross the lines $x_1 = x_2 = 0$. In general, from (36) it is seen that x_1 must be greater than zero whenever n is not an integer, and similarly, x_2 must be greater than zero whenever m is not an integer. This conclusion is exactly the same as the one drawn previously.

With the above restriction, the problem was solved for the reactor under consideration. Figure 7 shows the results for the diamond, square, and Euclidian norms. The broken lines give the respective values of δ, which are all equal in this case, and the solid lines show the corresponding stability regions. The symmetrical appearance of Figure 7 is due to the coincidental occurrence of values of $kc = 2$ for the square and diamond norms and $kc = \sqrt{2}$ for the Euclidian norm. While the size of both the square and the diamond is halved, the circle is only diminished by 0.707 and the figures become consecutively tangent. For all three cases, the limiting boundary of the ϵ condition is the x_1 axis (to avoid confusion, the other boundaries are not shown in Figure 7), and no further extension of the stability region can be obtained in the x_2 direction by this method. Even in the x_1 direction, only slight improvement is possible. Thus, it is apparent that coordinate transformations can do little to augment the region already found. The largest of the stability regions in Figure 7 comes from the Euclidian norm. On an absolute numerical scale, its size is diminutive, but on a physical basis it is quite substantial, since chemical conversions of species A from approximately 13% to 79%

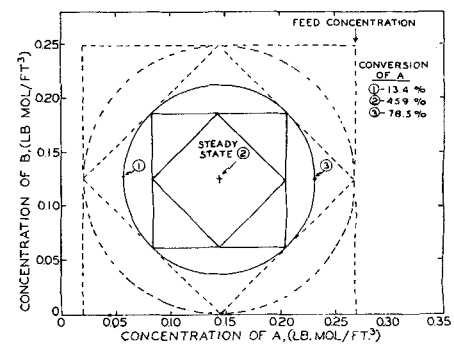

Fig. 7. Reversible isothermal reactor; stability regions for half-order reaction.

Table 4. Typical Stability Results for A Reversible Isothermal Reactor

Case number	n	m	x_{1_s}	x_{2_s}	Radius of stable region	Conversion at steady state (% A)	Conversion range in stable region (% A)
1	0.5	0.5	0.146	0.124	0.0879	45.9	13.4-78.5
2	0.5	1.5	0.130	0.140	0.0905	51.9	18.4-85.4
5	0.5	1.0	0.134	0.136	0.0935	50.4	15.7-85.0
7	1.5	1.0	0.229	0.041	0.162	15.2	0-75.2*
10	1.0	0.5	0.207	0.063	0.0444	23.3	6.9-39.6
12	2.0	0.5	0.254	0.016	0.0112	5.9	1.8-10.0
13	1.0	2.0	0.193	0.077	4.42	28.5	0-100*
14	2.0	1.0	0.247	0.023	0.887	8.5	0-100*
15	2.0	2.0	0.246	0.024	0.883	8.8	0-100*

* Range is larger, but not physically significant.
For all cases above, $K_F = 1.0$, $K_F = 0.2$, $\tau = 0.4$, $C_{Ao} = 0.270$, and $C_{Bo} = 0.0$.

are included in the stability region. The relative character of the terms "large" and "small" is emphasized by this example.

Representative results obtained with the Euclidian norm for various values of m and n are given in Table 4; a more complete summary is in Reference (5). In the first two cases listed, both m and n are nonintegral. Since the steady states are more or less equidistant from the coordinate axes, the corresponding stability regions are of a reasonable size. If, however, the system parameters were chosen so that a steady state were close to a coordinate axis, the circle of stability predicted would necessarily be small because of the restriction confining it to the first quadrant of the $x_1 - x_2$ plane. If one of the exponents in the rate expression is taken as an integer, the mathematical restraint in the corresponding direction is released, even though negative concentrations have no physical meaning. Examples of such situations are also given in Table 4. As long as one exponent remains nonintegral, the resulting stability region depends strongly on the position of the steady state. If, as in case 12, the steady state is close to the axis which cannot be crossed, the stability region is small. On the other hand, when it is far from the restraining axis, as in case 7, a large region results. This suggests that removal of all mathematical constraints should lead to extremely large regions. Cases 13 to 15 show this contention to be valid.

The stability regions found in this study compare favorably with those found by other methods and are quite practical. Furthermore, it should be emphasized in evaluating these results that very large stability regions for this problem may have limited physical significance, because the system equations include kinetic terms that are only valid over moderate ranges of temperature and concentration. On the other hand, the kinetic expressions used in the two examples developed here are among the simplest known, whereas practical kinetic data often fit very complicated expressions. In such situations, the use of the fundamental theorem is particularly advantageous because of its general applicability.

ACKNOWLEDGMENT

This research was supported by a grant from the National Science Foundation.

NOTATION

A_r = reactor area
$\mathbf{B}$ = transformation matrix
b_1, b_2 = constants defined in Equation (5)
c = constant in Equation (7)
C = effluent concentration
C_o = input concentration
C_o' = design input concentration
C_p = heat capacity
E = activation energy
$\mathbf{F}$ = vector whose elements are functions of the state variables
$\mathbf{f}$ = vector whose elements are defined in Equation (1)
$g_i(\mathbf{x})$ = nonlinear terms in $F_i(\mathbf{x})$
ΔH = heat of reaction
$\mathbf{J}$ = Jacobian matrix
k = constant in Equation (8)
k_o = frequency factor
k_1, k_2, k_3, k_4 = constants defined by Equation (21)
K_c, K_t = control constants defined by Equations (29) and (30)
K_F, K_R = constants defined in Equation (33)
n, m = constants defined by Equation (33)
Q = volumetric flow rate
q = constant defined by Equation (7)
R = gas constant
r = rate of removal of A by reaction per unit volume
s = subscript denotes evaluation at the steady state
T = effluent temperature
T_o = input temperature
T_a = ambient or coolant temperature
T_o' = design input temperature
t = time
U = overall heat transfer coefficient
$\mathbf{u}$ = state vector defined by Equation (4)
V = reactor volume
$\mathbf{x}$ = state vector
y = state vector defined as $(\mathbf{x} - \mathbf{x}_s)$

Greek Letters

α, β = stoichiometric coefficients
ρ = density
θ = angle of rotation used in coordinate transformation
τ = V/Q
$\psi(t)$ = principal matrix solution

LITERATURE CITED

1. Aris, R., and N. R. Amundson, *Chem. Eng. Sci.*, **7**, 121 (1958).
2. Bellman, R., "Stability Theory of Differential Equations," McGraw Hill, New York (1953).
3. Berger, J. S., and D. D. Perlmutter, *A.I.Ch.E. Journal*, **10**, 233 (1964).
4. ————, *Chem. Eng. Sci.*, **20**, 147 (1965).
5. Gura, Ira, Ph.D. Thesis, University of Illinois, 1964.
6. Hahn, W., "Theory and Application of Liapunov's Direct Method," Prentice-Hall, Englewood Cliffs, New Jersey (1963).
7. Hoftyzer, P. J., and T. N. Zwietering, *Chem. Eng. Sci.*, **14**, 241 (1961).
8. Kalman, R. E., and J. E. Bertram, *Am. Soc. Mech. Engrs. Trans.*, Series D, **82**, 371 (1960).
9. Nemytskii, V. V., and V. V. Stepanov, "Qualitative Theory of Differential Equations," Princeton University Press, Princeton, New Jersey (1960).
10. Struble, R. A., "Nonlinear Differential Equations," McGraw Hill, New York (1962).
11. Warden, R. B., R. Aris, and N. R. Amundson, *Chem. Eng. Sci.*, **19**, 149 (1963).

Manuscript received August 12, 1964; revision accepted December 30, 1964; paper accepted January 4, 1965.